

## Modeling of co- and early postseismic deformation due to the 2019 Ridgecrest earthquake sequence

Kang Wang (kwang@seismo.berkeley.edu) and Roland Bürgmann (burgmann@seismo.berkeley.edu)

Berkeley Seismological Lab., UC Berkeley

On July 4th, 2019, a Mw 6.4 earthquake struck the Searles Valley near the town of Ridgecrest in southern California. The Mw 6.4 earthquake was followed by a Mw 7.1 event about 34 hours later. Reports from field surveys and satellite imagery, including InSAR and optical images, indicate a complex network of faults activated by the 2019 Ridgecrest earthquakes. Here we use Sentinel-1 InSAR and GPS data to study the co- and early postseismic deformation due to this earthquake sequence. Since first postseismic SAR images from both ascending and descending tracks were taken after the Mw 7.1 earthquake, we invert for the combined coseismic slip due to both the Mw 6.4 and the Mw 7.1 earthquakes. The preferred slip model is characterized by a combination of left-lateral slip on a southwestward (SW) trending fault, which likely primarily ruptured during the Mw 6.4 foreshock, and right-lateral slip on a series of northwestward (NW) trending segments, which probably includes contributions from both events. The slip mostly concentrates in a depth range above 10 km, with a maximum slip of ~5 m. Assuming that the Mw 6.4 foreshock primarily ruptured the SW-trending fault, we find that the Mw 6.4 rupture imparted positive shear stress change and unclamping on the NW-trending faults near the Mw 7.1 hypocenter. Stress changes from both the Mw 6.4 and Mw 7.1 events appear to have significantly modulated the aftershocks and regional seismicity. Particularly, the Mw 7.1 mainshock produced stress shallows along the Mw 6.4 aftershock zones where the seismicity rate decreased dramatically after its occurrence. Relocated aftershocks reveal that south of the Mw 7.1 epicenter, where the rupture trace bifurcates, almost all aftershocks a few days after the mainshock occurred along a structure 3-4 km east of the main rupture surface trace. This is consistent with our geodetic inversion results that favor an east dipping fault segment along the main rupture trace that connects to the eastern branch at depth. We also observe clear near-field postseismic deformation one month after the mainshock. The early postseismic InSAR observations are characterized by subtle linear range change features across many of the fault traces, and significant deformation near junctions and stepovers of the fault segments. The postseismic deformation is indicative of both modest shallow afterslip and poroelastic rebound.

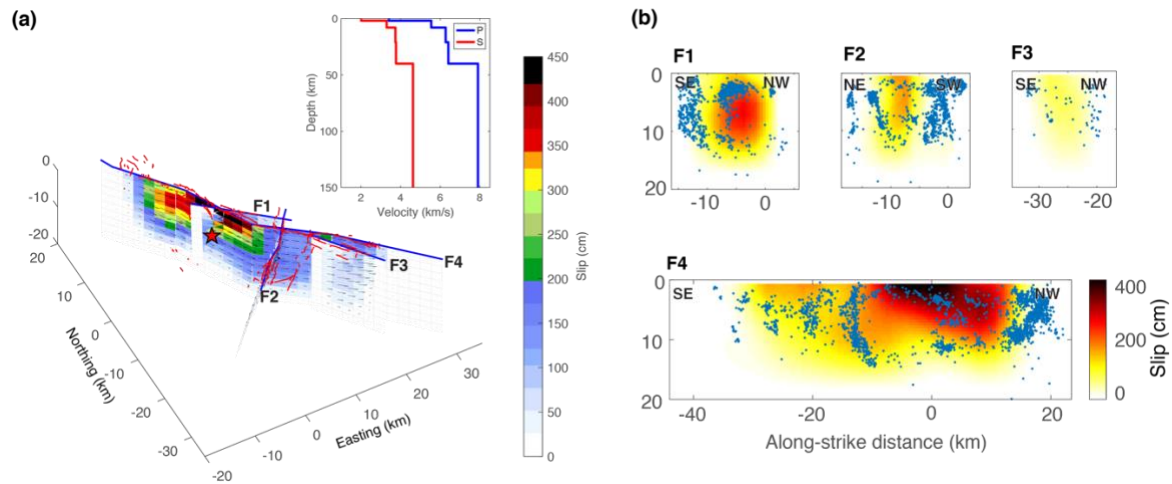


Figure 1. Coseismic slip model of the 2019 Ridgecrest earthquake sequence inverted from GNSS and Sentinel-1 InSAR data. (a) slip distribution in a 3-D perspective. Red lines represent surface traces of the 2019 Ridgecrest rupture verified by field survey (U.S. Geological Survey). Insert shows the seismic velocity structure for computing the Green's functions. (b) slip distribution along strike of the different fault segments. Dots are relocated aftershocks during ~5 days since the M6.4 event on 07/04 by David Shelly.

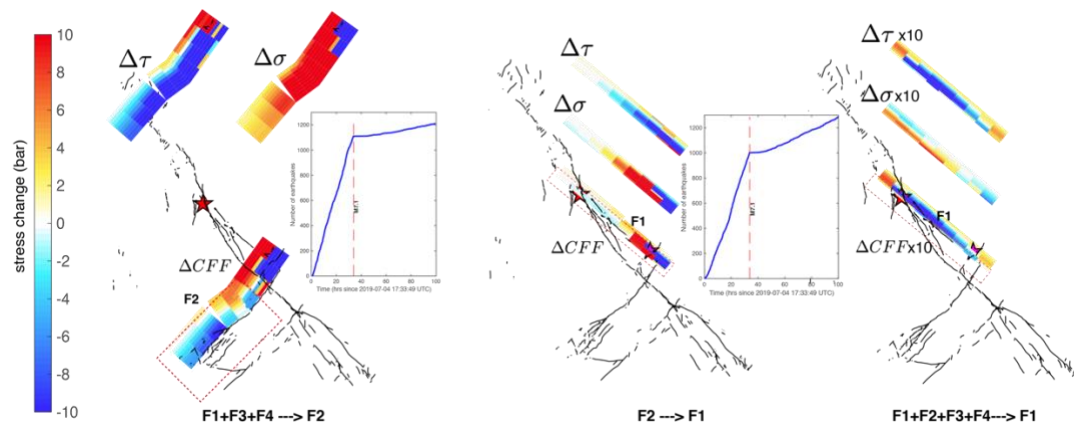


Figure 2. Stress interactions between fault segments based on the coseismic slip model shown in Figure 2. Text at the bottom of each panel indicates the 'source' and 'receiver' faults. For example,  $F1+F3+F3 \rightarrow F2$  represents that the source faults are F1, F2 and F3 (NW striking right-lateral), and the receiver fault is F2 (SW striking left-lateral). Note that total stress changes on F1 is a factor of 10 of what the colorbar shows. Inserts show the cumulative number of  $m < 2$  aftershocks along the respective receiver faults (marked by the red dash-line boxes).

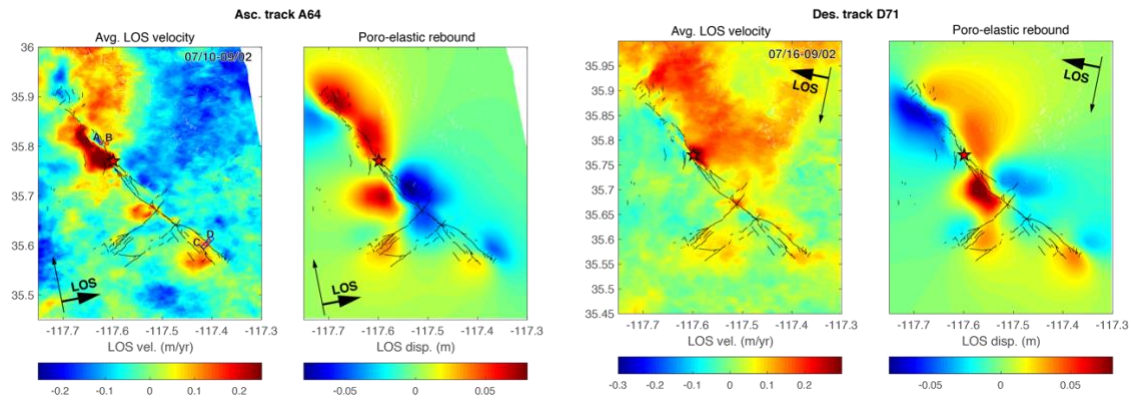


Figure 3. Postseismic InSAR velocity during first ~2 months and model predicted deformation due to the poroelastic rebound. We stacked all interferograms of temporal baselines < 35 days, after correcting for the atmospheric noises using GACOS products. No atmospheric noise correction was performed for the descending track D71. The calculation of poroelastic rebound is done with PEGRN/PECMP (Wang & Kümpel, 2003), assuming a poroelastic layer with hydraulic diffusivity of  $1 \text{ m}^2/\text{s}$ . The output is at 60 days after the earthquake.